Polymer 268 (2023) 125694

Contents lists available at ScienceDirect

Polymer

journal homepage: www.elsevier.com/locate/polymer

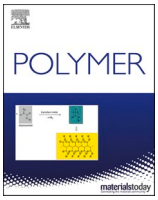

Steric hindrance affects interactions of poly(styrene–*alt*–DMHPMI) copolymer with strongly hydrogen-bond-accepting homopolymers

Wei-Ting Du [a], Tzu-Ling Ma [a], Shiao-Wei Kuo [a,b,*]

[a] Department of Materials and Optoelectronic Science, Center of Crystal Research, National Sun Yat-Sen University, Kaohsiung, 807, Taiwan
[b] Department of Medicinal and Applied Chemistry, Kaohsiung Medical University, Kaohsiung, 807, Taiwan

ARTICLE INFO

Keywords:
Hydrogen bonding
Steric hindrance
Alternating copolymers
Miscible blend

ABSTRACT

In this study, we synthesized the monomer *N*-(2,6-dimethylhydroxyphenyl)maleimide (DMHPMI) in three steps from 2,6-dimethylphenol and then reacted it with styrene through free radical copolymerization to prepare the alternating copolymer poly(styrene–*alt*–dimethylhydroxyphenylmaleimide) [poly(S–*alt*–DMHPMI)]. We used Fourier transform infrared (FTIR) spectroscopy, ^{1}H and ^{13}C nuclear magnetic resonance (NMR) spectroscopy, and mass-analyzed laser desorption ionization/time-of-flight (MALDI-TOF) mass spectrometry to confirm its structure. Differential scanning calorimetry revealed that blends of the alternating copolymers poly (S–*alt*–DMHPMI) and poly(styrene–*alt*–(*para*–hydroxyphenylmaleimide)) [poly(S–*alt*–*p*HPMI)] with the Strongly Hydrogen-Bond-Accepting homopolymers poly(4-vinylpyridine) (P4VP) and polyvinylpyrrolidone (PVP) each exhibited single-value glass transition temperatures (T_g) over the entire compositional range, indicative of full miscibility. Nevertheless, a negative deviation from the linear rule occurred for the T_g behavior of the PS–*alt*–PHPMI/P4VP blends, due to the weak acidity of the HPMI units, while the intermolecular interactions of the PS–*alt*–PHPMI coplymers were also inhibited because of strong self-association of the PHPMI units. FTIR spectral analyses of the ratio of hydrogen-bonded OH and pyridyl groups confirmed this behavior. In contrast, slightly positive deviations from the linear rule occurred for the T_g behavior when blending poly(S–*alt*–DMHPMI) or poly(S–*alt*–*p*HPMI) with the PVP homopolymer; here, the intermolecular interactions of the poly (S–*alt*–DMHPMI)/PVP blends were weaker than those of the poly(S–*alt*–*p*HPMI)/PVP blends, due to the steric hindrance of the DMHPMI units being greater than that of the *p*HPMI units.

1. Introduction

Introducing attractive intermolecular interactions can enhance the miscibility of polymer blends. For example, some polymers without polar functional groups [e.g., polypropylene (PP) and polystyrene (PS)] are immiscible with nylon, polyurethane (PU), and poly(4-vinylpyridine) (P4VP) [1–3]. As a result, the immiscible diblock copolymer PS-*b*-P4VP forms self-assembled nanostructure through a microphase separation mechanism [4–6]; introducing phenolic or acidic functional groups into the nonpolar polymer segment can enhance the miscibility [7–10]. The thermodynamic characteristics of polymer blends can be explained using the Flory–Huggins lattice theory [11,12], where the interaction parameter χ_{AB} represents the difference in the solubility parameters of polymers A and B, where London dispersion forces slightly influence the Gibbs free energy of the mixture. This approach cannot, however, explain the intermolecular interactions of polymer blend systems perfectly when hydrogen bonding is present; thus, Painter and Coleman added an extra term ($\Delta G_H/RT$) to the Flory–Huggins equation to accommodate the effect on the value of χ_{AB}, as follows:

$$\Delta G_{mix} / RT = \Phi_A \, ln \, \Phi_A/N_A + \Phi_B \, ln \, \Phi_B/N_B + \chi_{AB}\Phi_A\Phi_B + \Delta G_H/RT \qquad (1)$$

where ΔG_{mix} is the change in free energy of the polymer blend system, T is the temperature, R is the gas constant, and Φ_i and N_i are the volume fraction and segment number of each blend component, respectively. Even though the definition of a hydrogen bond is well established [13–15], controlling hydrogen bonds in polymer blends remains complicated. The factors affecting hydrogen bonding in polymers include the acidity and basicity of the proton donors and acceptors [16–20], steric effects, the bulk of the side groups, and the temperature

* Corresponding author. Department of Materials and Optoelectronic Science, Center of Crystal Research, National Sun Yat-Sen University, Kaohsiung, 807, Taiwan.
E-mail address: kuosw@faculty.nsysu.edu.tw (S.-W. Kuo).

https://doi.org/10.1016/j.polymer.2023.125694
Received 26 November 2022; Received in revised form 7 January 2023; Accepted 10 January 2023
Available online 13 January 2023
0032-3861/

[20–25].

For example, Pires et al. blended poly(ethylene oxide) (PEO) with novolac phenolic and polyvinylphenol (PVPh) and observed that the differences in acidity led to differences in the melting (T_m) and glass transition (T_g) temperatures of these two blend systems [17]. Coleman et al. found that increasing the length of the alkyl side groups of methacrylate units decreased the inter-association constant (K_A) significantly [22]. In a previous study, we observed the effects of steric hindrance on the hydrogen bonding ratio and the values of T_g when blending P4VP or poly(2-vinylpyridine) (P2VP) with phenolic; because the nitrogen atoms in P2VP are shielded by the main chain, these hydrogen bonded acceptor units are less readily accessed [20]. Furthermore, Fourier transform infrared (FTIR) spectra have revealed that bands representing the OH groups of PVPh and the C═O groups of polyvinylpyrrolidone (PVP) shifted to higher wavenumbers upon increasing the temperature, indicating that their hydrogen bonds were disrupted [26].

To enhance the miscibility of PS with P4VP, PVP, PEO or polycaprolactam (PCL) segments, OH groups can be incorporated randomly into the PS segment for interactions with the hydrogen bonded acceptor units. In this case, two factors should be considered when incorporating such hydrogen bond donor segments into nonpolar PS copolymers: the sequence distribution and steric effects. In this present study, we prepared hydroxyphenylmaleimide (HPMI) derivatives, instead of the typical phenolic units of PVPh, and examined the steric effects of their OH groups. In addition, intramolecular screening effect are known to influence the hydrogen bonding of copolymers [27–30]. Therefore, we performed free radical copolymerizations without protecting groups to obtain two poly(S–*alt*–PHPMI) copolymers—one containing dimethylhydroxyphenylmaleimide (DMHPMI) units and the other *p*HPMI units—and then blended them with P4VP and PVP homopolymers, respectively. We expected intermolecular hydrogen bonding to occur between the OH units of these two PHPMIs and the pyridyl units of P4VP and the C═O units of PVP; we chose these two homopolymers because P4VP and PVP have high values of K_A (1200 and 6000, respectively) when blended with PVPh. We used ^{1}H and ^{13}C NMR spectroscopy, FTIR spectroscopy, and MALDI-TOF mass spectrometry to confirm the chemical structure and sequence distribution of the PS–*alt*–DMHPMI alternating copolymer and investigate its hydrogen bonding interactions with the homopolymers. We obtained miscible polymer blends for P4VP and PVP with these two PS–*alt*–PHPMI copolymers, as evidenced using differential scanning calorimetry (DSC). One-dimensional (1D) and two-dimensional (2D) FTIR spectroscopy allowed us to explore the hydrogen bonding interactions in these PS–*alt*–PHPMI/P4VP and PS–*alt*–PHPMI/PVP blends.

2. Experimental section

2.1. Materials

Tin(II) chloride dihydrate ($SnCl_2{\cdot}2H_2O$, 98%), maleic anhydride (98%), styrene (99%), hydrochloric acid (HCl, 35.5–36.5%), and PVP (M_n = 58,000 g/mol) were acquired from Alfa Aesar. Sodium nitrite ($NaNO_2$, 98.5%), azobisisobutyronitrile (AIBN), magnesium sulfate anhydrous ($MgSO_4$, 99%), and *p*-toluenesulfonic acid monohydrate ($TsOH{\cdot}H_2O$, 99%) were purchased from SHOWA. 2,6-Dimethylphenol (99%), 4-vinylpyridine (95%), tetrahydrofuran (THF), methanol (MeOH), ethanol (EtOH, 99.5%), 2-propanol (IPA), diethyl ether (Et_2O), hexane, dichloromethane (DCM), ethyl acetate (EA), and toluene were obtained from Acros Organics. Sodium carbonate (Na_2CO_3), sodium bicarbonate ($NaHCO_3$), and *N*,*N*-dimethylformamide (DMF) were acquired from J. T. Baker. The syntheses of *p*HPMI and poly(S–*alt*–*p*HPMI) have been described previously [25].

2.2. Characterization

^{1}H and ^{13}C NMR spectra were recorded using an INOVA 500 spectrometer, with chloroform-*d* or DMSO-d_6 as an external standard. FTIR spectra were recorded using a Bruker Tensor 27 FTIR spectrophotometer and the conventional crystal KBr disk method; 32 scans were collected at a spectral resolution of 4 cm^{-1}; a temperature-controlled compartment holder was used to record FTIR spectra at various temperatures under a N_2 atmosphere to maintain dry sample films. Mass spectra of the HPMI derivatives were recorded using a Bruker Daltonics Autoflow MALDI-TOF mass spectrometer. Molecular weights were determined using a Bruker Solarix high-resolution Fourier transform mass spectrometry system. Melting points and glass transition temperatures were measured using a TA Q–20 differential scanning calorimeter, with ca. 5 mg of sample placed on the DSC sample pan under a N_2 atmosphere (100 mL min^{-1}), with heating from 40 to 300 °C at a heating rate of 10 °C min^{-1}. Weight-average (M_w) and number-average (M_n) molecular weights and polydispersity indexes (M_w/M_n) were determined using GPC (Waters 510 gel permeation chromatograph).

2.3. 2,6-Dimethylbenzoquinone 4-oxime (DMBQ)

$NaNO_2$ (1.50 g) was added to a solution of 2,6-dimethylphenol (14.69 mmol) in HCl (10 mol L^{-1}, 10 mL) and EtOH (10 mL) at 0 °C and then the mixture was kept cool while stirring for 1 h. EtOH (2 mL) was added and then the mixture was kept at room temperature with 1 h. The solution was poured into water and the aqueous phase extracted with Et_2O. The organic phase was extracted with aqueous Na_2CO_3 (10 wt%). Acidification of the carbonate solution with HCl (3 mol L^{-1}) provided a yellow precipitate, which was collected, washed with hexane, and dried [31]. Yield: 81%; m.p. 175 °C; FTIR (KBr, cm–1): 2770–3000 (alkane C–H stretching), 1605 (C═C, aromatic ring); 1H NMR (500 MHz, chloroform-d, δ, ppm): 2.05 (s, 3H, CH_3), 2.09 (s, 3H, CH_3), 7.00 (s, 1H, ArH), 7.56 (s, 1H, ArH).

2.4. 4-Amino-2,6-dimethylphenol (DMAP)

A mixture of 2,6-dimethylbenzoquinone 4-oxime (3.15 mmol), $SnCl_2{\cdot}2H_2O$ (2.15 g, 9.50 mmol), DCM (30 mL), and concentrated HCl (0.6 mL) was heated under reflux at 60 °C for 2 days. The DCM was evaporated under vacuum and the residue extracted with concentrated aqueous $NaHCO_3$. The organic phase was concentrated under vacuum to obtain a burgundy solid [31]. Yield: 59%; m.p. 140 °C; FTIR (KBr, cm–1): 3359 (N–H asymmetric stretching), 3291 (N–H symmetric stretching), 1613 (C═C, aromatic ring); 1H NMR (500 MHz, chloroform-d, δ, ppm): 6.73 (s, 2H, ArH), 2.21 (s, 6H, CH3).

2.5. N-(2,6-Dimethylhydroxyphenyl)maleimide (DMHPMI)

Maleic anhydride (4.00 g, 40.8 mmol) and 4-amino-2,6-dimethylphenol (4.36 g, 40.0 mmol) were dissolved in DMF (15 mL) and toluene (70 mL) in a 125-mL round-bottom flask and stirred for 10 min at room temperature. Adequate DMF containing a trace amount of $TsOH{\cdot}H_2O$ was added into the flask dropwise and then the solution was heated under reflux for 2 days. The resulting solution was cooled in an ice bath and cold water was added. The solid was filtered off, washed with water, recrystallized from IPA, and dried under vacuum at 70 °C for 24 h to give light-brown needles. This method is similar with ref [25]. Yield: 30%; m.p. 193 °C; FTIR (KBr, cm–1): 3455 (OH), 1705 (C═O); 1H NMR (500 MHz, chloroform-d, δ, ppm): 2.26 (s, 6H, CH3), 6.82 (s,2H, ArH), 6.90 (s, 2H, =CH); 13C NMR (125 MHz, chloroform-d, δ, ppm): 16.03 (CH3), 123.46–127.51 (ArC), 134.82 (=CH), 153.00 (COH), 170.95 (C═O).

2.6. Poly(S–alt–DMHPMI) alternating copolymers

DMHPMI (0.652 g, 3.00 mmol) and AIBN (5 wt%) were placed in a 100-mL three-necked round-bottom flask. Dry THF (18.8 mL) and

styrene (0.313 g, 3.00 mmol) were injected into the flask and then the mixture was stirred under N_2 at 70 °C for 24 h. The copolymerization was quenched by exposing the solution to air for 30 min. The solution was added dropwise into cold MeOH and the solid was reprecipitated at least three times from cold THF/MeOH. The solid was dried for 3 days at 50 °C under vacuum to remove any residual solvent. This method is similar with ref [25]. Yield: 0.554 g; FTIR (KBr, cm–1): 3490 (OH), 1705 (C═O); 1H NMR (500 MHz, DMSO-d_6, δ, ppm): 2.09 (s, 6H, CH3), 5.98–7.56 (m, 7H, ArH), 8.51 (s, 1H, OH); 13C NMR (125 MHz, DMSO-d_6, δ, ppm): 16.53 (CH3), 123.32–129.21 (ArC), 153.96 (COH), 176.40–179.20 (C═O); number-average molecular weight (Mn): ca. 46, 000 g mol^{-1} (Fig. S1).

2.7. Poly(4-vinylpyridine) (P4VP)

AIBN (5 wt%) were placed in a 100-mL three-necked round-bottom flask. Dry THF (23 mL) and 4-vinylpyridine (1.00 g, 9.50 mmol) were injected into the flask and then the mixture was stirred under N_2 at 70 °C for 24 h. The polymerization was quenched by exposing the solution to air for 30 min. The solution was added dropwise into cold Et_2O and the solid was reprecipitated at least three times from cold MeOH/Et_2O. The solid was dried for 3 days at 50 °C under vacuum. Yield: 0.718 g; FTIR (KBr, cm–1): 3028 (aromatic C–H stretching), 2930 (alkane C–H stretching), 1597 (C═N), 993 (aromatic C–H bending); 1H NMR (500 MHz, DMSO-d_6, δ, ppm): 1.20–2.00 (3H, CH2CH), 6.60 (2H, C═CH in pyridine), 8.26 (2H, N═CH in pyridine); 13C NMR (125 MHz, DMSO-d_6, δ, ppm): 42.54 (CH2CH), 123.52–154.24 (pyridine ring C atoms); number-average molecular weight (Mn): ca. 77,360 g mol^{-1} (Fig. S5).

2.8. Blend preparation

Blending of P4VP or PVP with poly(S–*alt*–*p*HPMI) or poly (S–*alt*–DMHPMI) was performed through solution-casting. The components were dissolved in DMF at 5 wt%, stirring overnight to ensure a homogeneous solution. The solvent was evaporated over 3 days at 40 °C and the residual DMF was evaporated under vacuum at 70 °C for 2 days.

3. Results and discussion

3.1. Synthesis of DMHPMI monomers

We prepared the DMHPMI monomer through numerous synthesis steps [Fig. 1(a)] because 2,6-dimethylaminophenol is not commercially available [31]. We synthesized 2,6-dimethylbenzoquinone 4-oxime from 2,6-xylenol. Because of the tautomerization between the oxime group and the nitroso-phenol unit, FTIR spectroscopy revealed that 2, 6-dimethylbenzoquinone 4-oxime featured a broader O–H stretching mode, relative to the single sharp stretching mode of 2,6-xylenol [32], as displayed in Fig. 1(b). ^{1}H NMR spectroscopy revealed two signals for the methyl groups at 2.05 and 2.09 ppm, consistent with their different chemical environments, as well as singlets at 7.00 and 7.56 ppm for the protons on the aromatic ring, indicating that the hydrogen atom at the para position had been replaced [Fig. 1(c)]. We obtained 2,6-dimethylaminophenol after reducing 2,6-dimethylbenzoquinone 4-oxime with stannous chloride. Signals for the amino group at 3291 and 3359 cm^{-1} appeared in the FTIR spectrum in Fig. 1(b); the symmetry of the chemical structure was revealed by the signal of the methyl groups being a singlet at 6.73 ppm by the ^{1}H NMR spectrum [Fig. 1(c)]. Finally, we

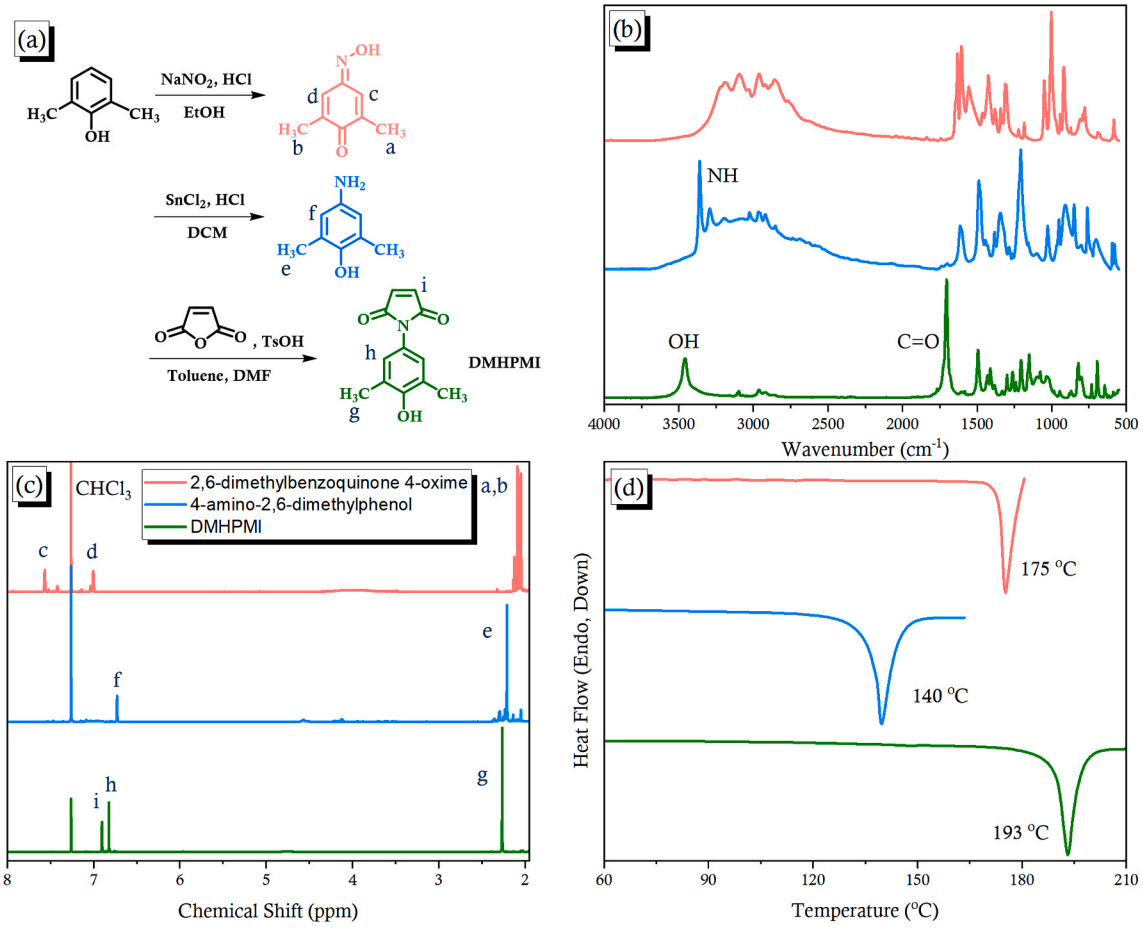

Fig. 1. (a) Synthesis of 2,6-dimethylbenzoquinone 4-oxime, 4-amino-2,6-dimethylphenol, and the DMHPMI monomer. (b–d): (b) FTIR spectra, (c) ^{1}H NMR spectra, and (d) DSC thermal analyses of 2,6-dimethylbenzoquinone 4-oxime, 4-amino-2,6-dimethylphenol, and DMHPMI monomer.

reacted maleic anhydride and 2,6-dimethylaminophenol to obtained DMHPMI, which featured a single O–H stretching mode at 3455 cm^{-1} in its FTIR spectrum and three different chemical environments for its hydrogen atoms (singlets at 2.26, 6.82 and 6.90 ppm) in its ^{1}H NMR spectrum; furthermore, its melting point was significantly different from that of the starting material [Fig. 1(d)]. In addition, we synthesized *p*HPMI by using a method described previously [25].

3.2. Synthesis of PS–alt–PHPMI copolymers

We prepared poly(S–*alt*–DMHPMI) and poly(S–*alt*–*p*HPMI) copolymers through free radical copolymerizations of styrene with the respective HPMI monomers [Fig. 2(a)]. Their chemical structures were confirmed using FTIR and NMR spectroscopy and MALDI-TOF mass spectrometry. The FTIR spectrum of poly(S–*alt*–DMHPMI), recorded after removing all moisture [Fig. 2(b)], featured strong signals for its OH and C═O groups. The signal for the OH groups of poly(S–*alt*–DMHPMI) appeared at 3490 cm^{-1}, a wavenumber higher than that of 3450 cm^{-1} for poly(S–*alt*–*p*HPMI); furthermore, the full width at half maximum (FWHM) of the OH absorption was narrower than that of poly (S–*alt*–*p*HPMI) [Fig. 2(c)]. The FWHM of the signal for C═O stretching of poly(S–*alt*–DMHPMI) was also less than that of poly(S–*alt*–*p*HPMI) [Fig. 2(d)]. These features suggested that the intra- and/or intermolecular hydrogen bonding in poly(S–*alt*–DMHPMI) was relatively weak [33]. The ^{1}H NMR spectrum of poly(S–*alt*–DMHPMI) [Fig. 2(e)] featured signals at 2.09, 5.98–7.56, and 8.51 ppm representing its methyl, aromatic, and OH protons. Its ^{13}C NMR spectrum (Fig. S4) featured signals at 16.53, 123.32–129.21, 153.96, and 176.40–179.20 ppm for the methyl, aromatic, C–OH, and C═O units, respectively. Poly (S–*alt*–*p*HPMI) has been copolymerized previously [25]. Gel permeation chromatography (GPC) revealed significant aggregation in the column, arising from significant hydrogen bonding of the *p*HPMI units, resulting in a bimodal distribution (Fig. S1); in comparison, a single peak appeared for poly(S–*alt*–DMHPMI), suggesting weaker hydrogen bonding.

We used the ^{1}H NMR spectra to determine the DMHPMI/styrene repeat unit ratios in the alternating copolymer poly(S–*alt*–DMHPMI), by integrating the signals of the OH groups and aromatic units. The DMHPMI/styrene repeat unit ratio was 1:0.92, whereas the *p*HPMI/styrene repeat unit ratio was 1:1.15 [25]; these values are reasonable for alternating copolymers. The MALDI-TOF mass spectrum in Fig. 2(f) provides evidence suggesting that the poly(S–*alt*–DMHPMI) copolymer was a near-perfect alternating copolymer with equal numbers of HPMI units and styrene units [34–36]. The difference between the signals at *m/z* 5461.32 and 5783.49 was approximately 321 g mol^{-1}, equal to the summed molecular weight of one styrene and one DMHPMI unit. Furthermore, there were 18 units of DMHPMI (18 × 217.22 u) and 18 units of styrene (18 × 104.15 u) for the signal labeled 18:18. The other

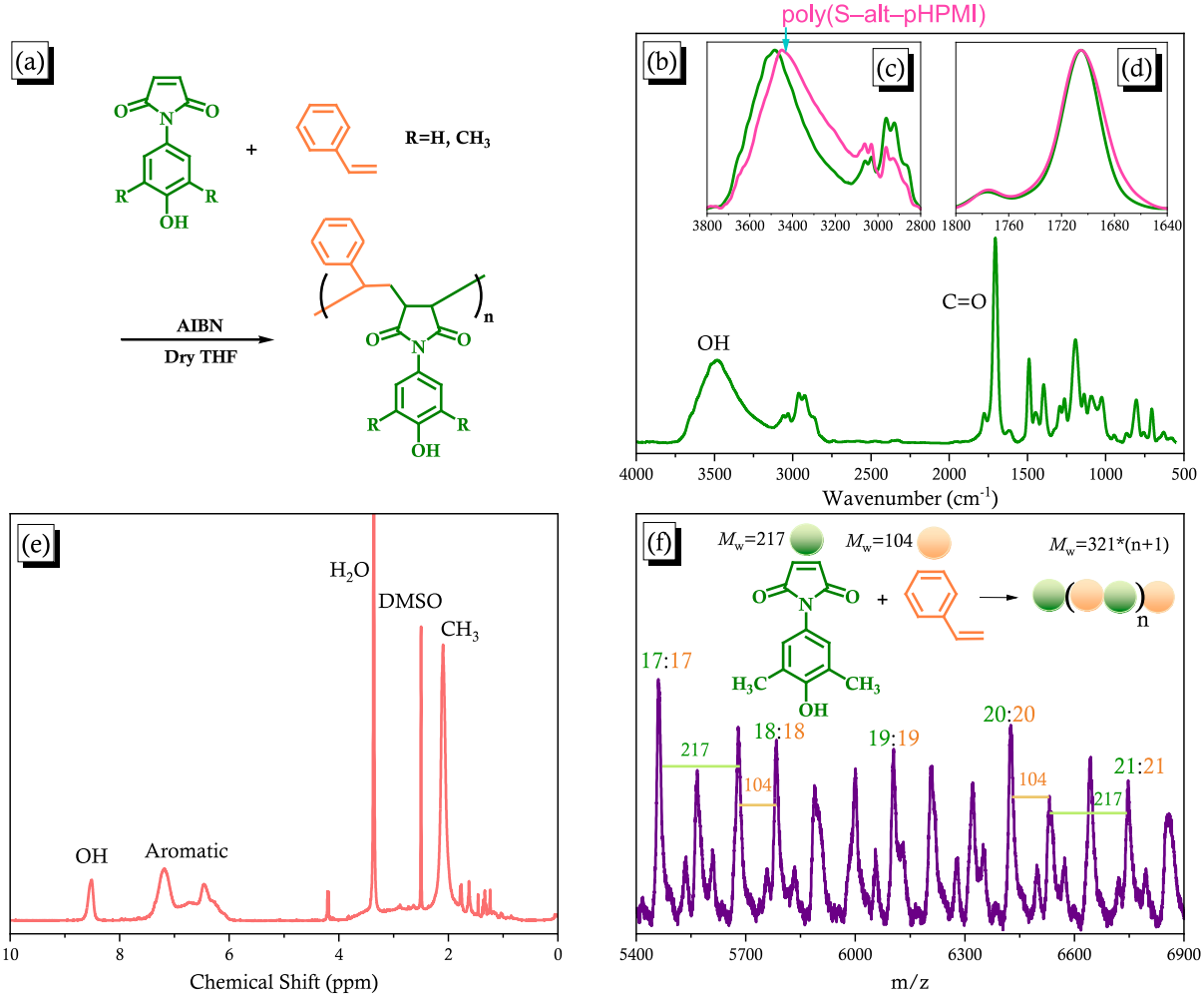

Fig. 2. (a) Synthesis of the alternating copolymer PS–*alt*–PHPMI. (b) FTIR spectra of poly(S–*alt*–DMHPMI). (c) Expanded-view FTIR spectra displaying the region of the OH groups of poly(S–*alt*–DMHPMI) and poly(S–*alt*–*p*HPMI). (d) Expanded-view FTIR spectra displaying the region of the C═O group of poly(S–*alt*–DMHPMI) and poly(S–*alt*–*p*HPMI). (e) ^{1}H NMR spectrum of poly(S–*alt*–DMHPMI). (f) MALDI-TOF mass spectrum of poly(S–*alt*–DMHPMI), with the molecular weights of the styrene and DMHPMI units.

intense signals in the spectrum of poly(S-*alt*-*p*HPMI) correspond to perfectly alternating sequences with DMHPMI:styrene ratios of *n*–1:*n*, *n*:*n*–1, and *n*:*n* (e.g., 17:18, 18:17, and 18:18, respectively). The other residues were difficult to count, owing to the presence of DCTB as the matrix [37].

3.3. Analyses of PS–alt–PHPMI/P4VP blends

The ratio of the association constants K_A/K_B is more important than the absolute values of K_A and K_B; it can be calculated from the change in free energy of mixing, with the value of K_A of the polymer blend determined from the values of K_2 and K_B (the dimer and multimer self-association constants, respectively) [15]. The intermolecular interaction would be stronger if the value of K_A were greater and/or the value of K_B were lower. First, we selected P4VP, polymerized through free radical reaction, as the hydrogen bond acceptor; it has a higher value of K_A than most other homopolymers. Fig. S5 provides characterization data confirming its chemical structure; the number-average molecular weight was approximately 77,000 g/mol, and its glass transition temperature (131 °C) was similar to previous reports [20,23]. The values of K_2 and K_B of a 2,6-xylenol unit (6.7 and 24.5) are lower than those of a phenol unit (21.0 and 66.8), as claimed by the Coleman group [38].

Fig. 3(a) and (b) present the DSC thermograms of a diverse set of poly(S–*alt*–DHPMI)/P4VP and poly(S–*alt*–*p*HPMI)/P4VP blends. The pure poly(S–*alt*–DMHPMI) (T_g = 242 °C) and poly(S–*alt*–*p*HPMI) (T_g = 259 °C) alternating copolymers had values of T_g higher than those of PS–*co*–PVPh copolymers possessing various PVPh compositions (reported to be approximately 100–180 °C) [39]. Without a hydrogen-bond donor, the value of T_g of the styrene–maleic anhydride (SMA) alternating copolymer (184 °C) is also higher than that of PS–*co*–PVPh copolymers, because the backbone of the maleic anhydride unit restricts the degree of freedom [40]. Moreover, the values of T_g of the PS–*alt*–PHPMIs were higher than that of the SMA, due to the hydrogen-bonded donor units on the side chains. The single value of T_g for each of the binary blends suggested that their components possessed miscibility in the amorphous phase. Notably, each value of T_g for the poly(S–*alt*–DMHPMI)/P4VP blends was lower than that of the poly(S–*alt*–*p*HPMI)/P4VP blends, and even lower than the value of T_g of the pure alternating copolymer. Interestingly, when we used the Kwei equation [41] to fit the results [summarized in Fig. 3(c) and (d)], we found that both blends featured negative deviations from the linear rule. For the poly(S–*alt*–DMHPMI)/P4VP blends, we obtained values of *k* and *q* of 1 and –105, respectively; for the poly(S–*alt*–*p*HPMI)/P4VP blends, these values were 1 and –95, respectively. Negative values of *q* are rare for P4VP blends with PVPh homopolymers or PVPh-based copolymers. For example, PVPh/P4VP blends (q = 100) [42], the PVPh-*b*-P4VP copolymer (q = 185), and other PVPh-based copolymer/P4VP blends (q = 111–186) [43] have displayed positive values of *q*, because the value of K_A of the PVPh/P4VP blend (1200) is significantly larger than the value of K_B of pure PVPh (66.8). Therefore, self-association of the OH and C═O groups of HPMI derivatives would enhance the value of K_B of DMHPMI or *p*HMPI and, thus, we would expect the ratio K_A/K_B to decrease significantly and the value *q* to decrease.

To investigate the reason why the poly(S–*alt*–DMHPMI)/P4VP blends featured a more negative deviation in its value of *q*, and opposite to previous expectations, we examined the hydrogen bonding interactions in the poly(S–*alt*–DMHPMI)/P4VP and poly(S–*alt*–*p*HPMI)/P4VP binary blends through FTIR spectra recorded at 25 °C after removing moisture. The symmetric and asymmetric stretching signals of the maleimide units, at 1712–1716 and 1775–1778 cm^{-1}, respectively, featured two signals for the C═O absorptions of the two pure PS–*alt*–PHPMI copolymers. The band widths and shapes of the C═O

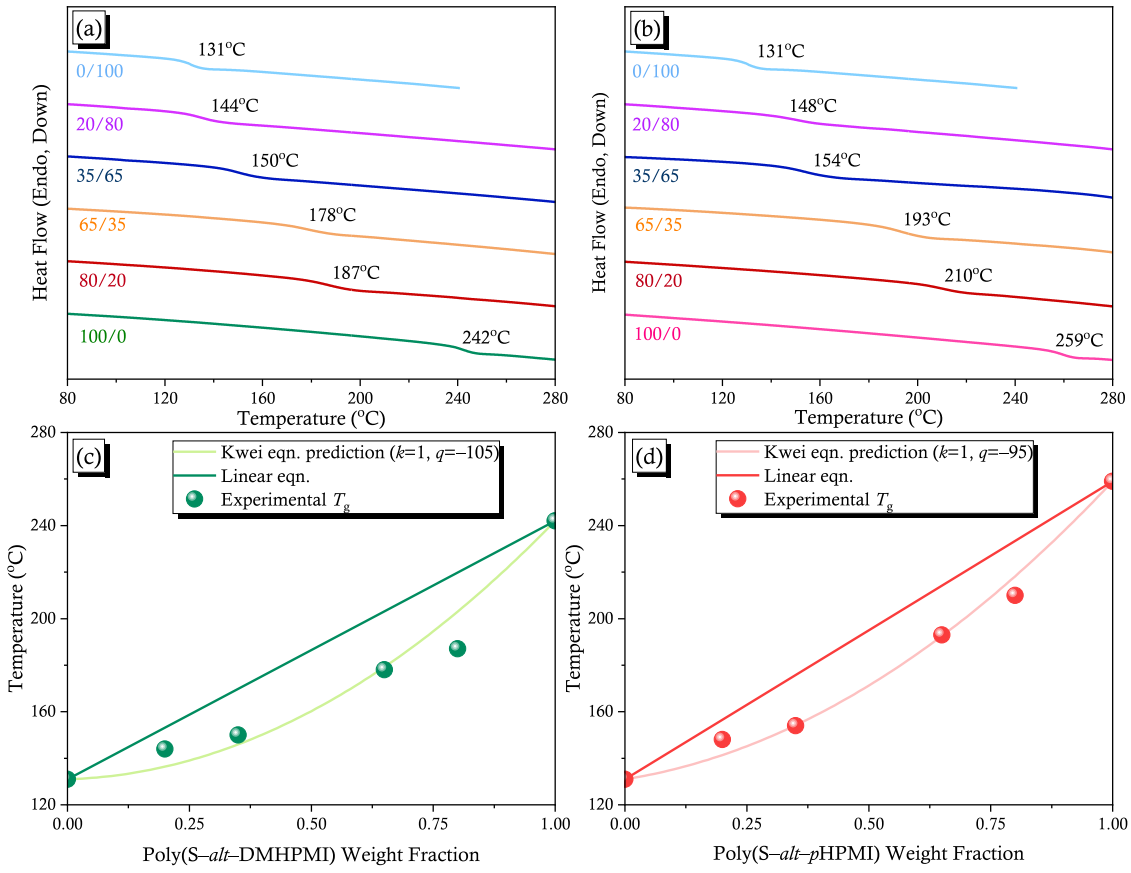

Fig. 3. (a, b) DSC thermal analyses of (a) poly(S–*alt*–DMHPMI)/P4VP and (b) poly(S–*alt*–*p*HPMI)/P4VP binary blends of various weight ratios. (c, d) Corresponding values of T_g predicted by the linear rule and the Kwei equation for the (c) poly(S–*alt*–DMHPMI)/P4VP and (d) poly(S–*alt*–*p*HPMI)/P4VP binary blends.

signals recorded at different poly(S–*alt*–DMHPMI)/P4VP blends ratios were similar [Fig. 4(a)]. In contrast, Fig. 4(c) reveals that the C═O signals widened upon increasing the poly(S–*alt*–*p*HPMI) content. There is the more obvious difference on Fig. S6. The FWHM of the signal for the C═O groups in the pure poly(S–*alt*–*p*HPMI) was narrower than those for the 80/20 and 65/35 poly(S–*alt*–*p*HPMI)/P4VP binary blends, because the intramolecular (or self-association) interactions of poly (S–*alt*–*p*HPMI) were stronger than the intermolecular interactions between this copolymer and P4VP ($K_B > K_A$). Similar phenomena, with a negative deviation from the linear rule, have been reported previously [44–46]. To the best of our knowledge, however, this paper is the first to report a blending system with P4VP, a strong hydrogen bond acceptor, displaying a negative deviation from the linear rule [23,27,47].

On the other hand, the bands of the pyridine ring were sensitive to any intermolecular interactions between the OH and pyridyl units, including the signals at 1597 and 993 cm^{-1} for P4VP [28]. Unfortunately, the band at 1597 cm^{-1} was too close the signal of the aromatic rings to observe, so we could use only the band at 993 cm^{-1} of pure P4VP to observe the intermolecular interactions. We assigned the band at 1005 cm^{-1} to the hydrogen-bonded pyridine rings [28]. Fig. 4(b) reveals that the intensity of hydrogen-bonded band increased slightly upon increasing the poly(S–*alt*–DMHPMI) content, whereas a relatively large increase occurred for the band at 1005 cm^{-1} for the poly (S–*alt*–*p*HPMI)/P4VP binary blends [Fig. 4(d)]. Fig. 4(e) summarizes the variations of the fractions of hydrogen-bonded N atoms of P4VP and the FWHMs of the C═O groups of the copolymers. For the.

poly(S–*alt*–DMHPMI)/P4VP binary blends, these two parameters remained constant, whereas there were obviously increasing trends

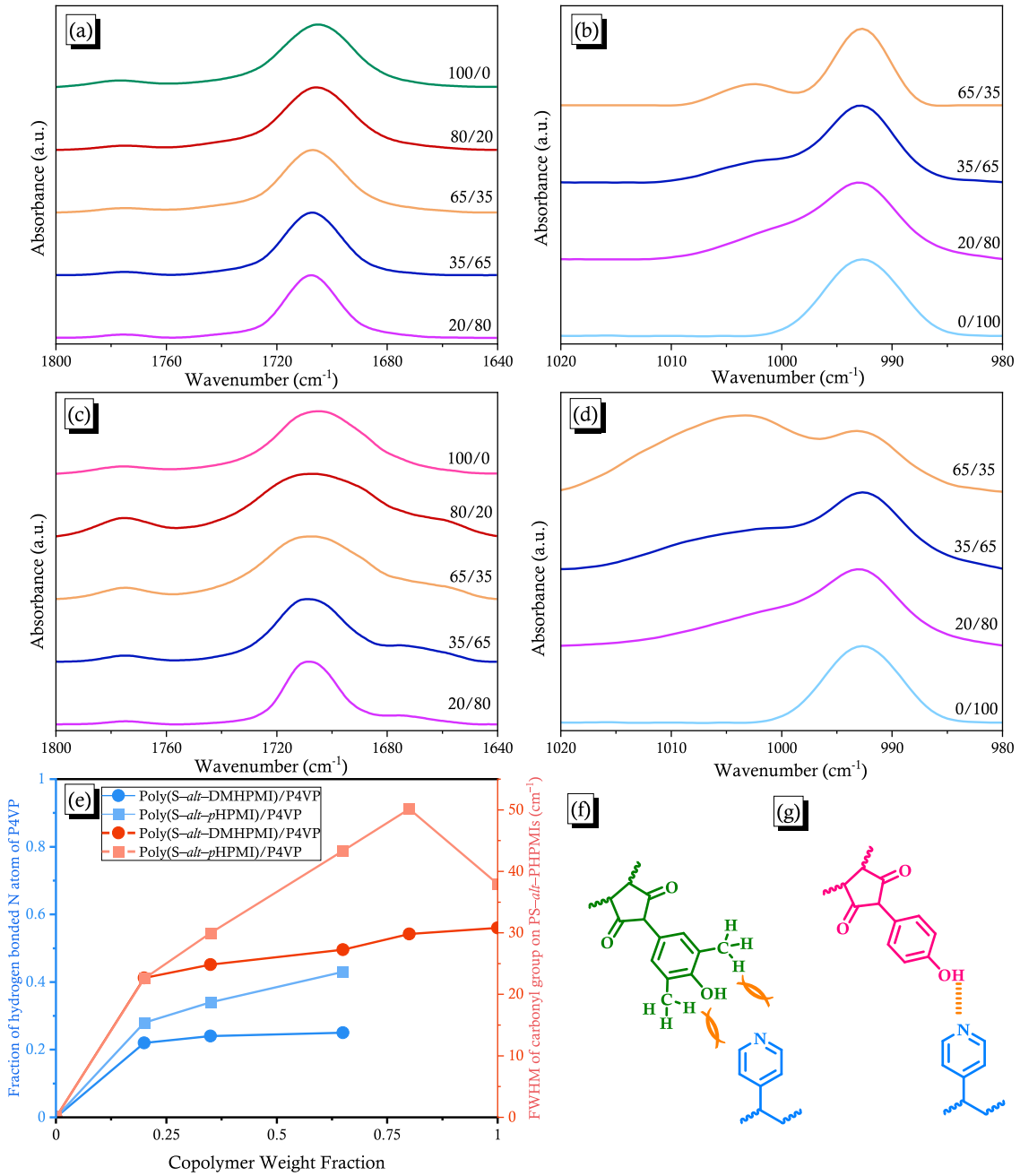

Fig. 4. (a, c) C═O group stretching and (b, d) pyridyl C–H bending regions in the FTIR spectra of (a, b) poly(S–*alt*–DMHPMI)/P4VP and (c, d) poly(S–*alt*–*p*HPMI)/P4VP binary blends recorded at 25 °C after removing moisture. (e) Fractions of hydrogen-bonded N atoms of P4VP and FWHMs of the signals of the C═O groups in the PS–*alt*–PHPMIs. (f, g) The scheme of DMHPMI unit interacting with P4VP (f) and *p*HPMI unit interacting with P4VP (g).

upon increasing the content of poly(S–*alt*–*p*HPMI), indicating that the OH groups of poly(S–*alt*–*p*HPMI) were stronger hydrogen-bond donors than those of poly(S–*alt*–DMHPMI). In addition, the hydrogen bonding ratios in both binary blends were much lower than those in PVPh/P4VP binary blends [26], because of the lower acidities of both hydrogen bond donors, with the resonance effect of the N atom of the maleimide unit making it weaker than a phenol unit. In summary, the methyl group hindered the OH group from interacting with the N atoms of P4VP, due to the steric bulk of the DMHPMI unit [Fig. 4(f)], while the acidity of the hydrogen bond donor also influenced the intermolecular interaction even in the absence of any steric bulk beside the OH group [Fig. 4(g)].

To determine the various hydrogen bonding strengths in both binary blends, we investigated whether the intermolecular interactions between these alternating copolymers and P4VP were influenced by the temperature, using a weight ratio of 65/35. The band for the C═O group was almost unchanged upon the increasing temperature of the PS–*alt*–PHPMI/P4VP binary blends [Fig. 5(a) and (c)], but the ratio of hydrogen-bonded pyridine rings decreased, indicating that most of the hydrogen bonding was between the OH groups and the N atoms of the pyridine rings [Fig. 5(b) and (d)]. We confirmed the FTIR spectral bands for the hydrogen-bonded pyridine rings and pure P4VP through 2D FTIR spectral analysis, a powerful method that we have used previously [45], as established by the Noda group [48]. Fig. 5(e) presents the synchronous 2D IR correlation map for the N atoms on the pyridine rings at 980–1200 cm^{-1}. The signal for the N atoms on the pyridine units in pure P4VP was located at 993 cm^{-1}; for the intermolecularly hydrogen-bonded N atoms on the pyridine units, it was located at 1005 cm^{-1}. Negative cross-peaks appeared for the signals at 993 and 1005 cm^{-1}, demonstrating that these two absorption bands varied in opposite directions: one was for the free N atoms in pyridine rings and the other was for the hydrogen-bonded functional groups, as expected. The asynchronous 2D correlation map in Fig. 5(f) features negative cross-peaks in the upper left (993 vs. 1005 cm^{-1}) that display the same behavior as that in the synchronous graph; therefore, the band at 1005 cm^{-1} was altered prior to the band at 993 cm^{-1}. This behavior is reasonable because a hydrogen-bonding interaction is more sensitive to an increase in temperature than that of an N atom of a pyridine ring, thereby resulting in a later response for a free N atom of a pyridine ring.

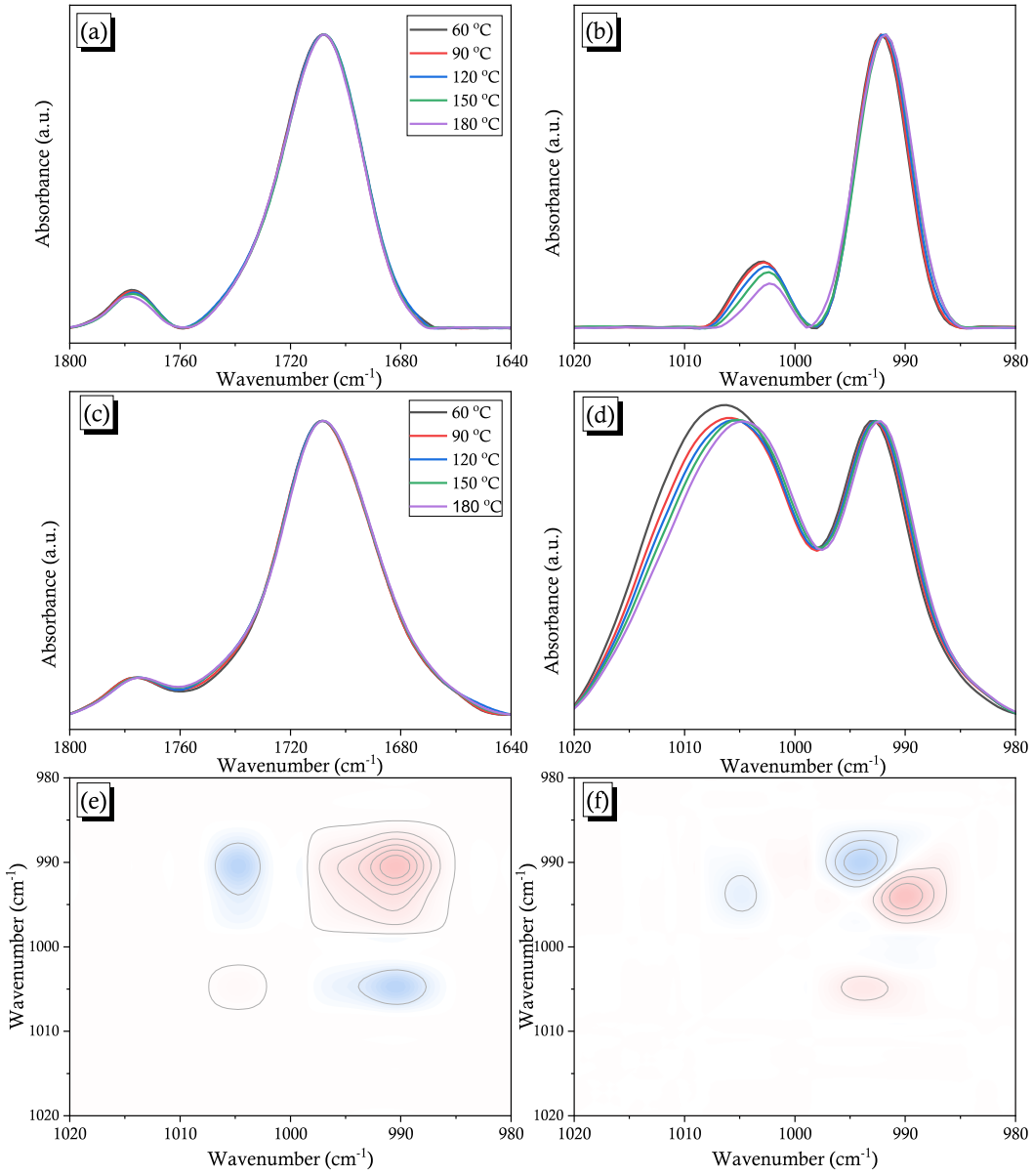

Fig. 5. (a–d) FTIR spectra of the (a, c) C═O and (b, d) pyridyl C–H bending regions, recorded from 60 to 180 °C, for the 65/35 ratio (a, b) poly(S–*alt*–DMHPMI)/P4VP and (c, d) poly(S–*alt*–*p*HPMI)/P4VP blends. (e, f) 2D FTIR spectral (e) synchronous and (f) asynchronous correlation maps.

These findings suggested the OH groups of the DMHPMI and *p*HPMI units attracted the pyridine rings primarily, and affected the C═O groups only slightly.

3.4. Analyses of PS–*alt*–PHPMI/PVP blends

Although we observed a negative deviation from the linear rule for the PS–*alt*–PHPMI/P4VP binary blends in Fig. 3, a positive deviation from the linear rule occurred for the poly(S–*alt*–*p*HPMI)/PVP binary blends in Fig. S8 [25]. Fig. 6 presents the interesting behavior of the poly (S–*alt*–DMHPMI)/PVP binary blends. We observed only a single value of T_g for each blend ratio, indicating that poly(S–*alt*–DMHPMI) was miscible with PVP at various ratios [Fig. 6(a)]. In particular, we obtained a positive deviation ($k = 1$, $q = 40$) from the linear rule when using the Kwei equation [Fig. 6(b)], in contrast of the negative deviation for the poly(S–*alt*–DMHPMI)/P4VP blends, due to notably different values of K_A of 1200 for P4VP and 6000 for PVP, as revealed previously in the literature [38]. Fig. 6(c) presents the signals of the C═O groups of the DMHPMI units with asymmetric and symmetric stretching; the signals for C═O stretching in PVP appeared at 1775, 1705, and 1680 cm^{-1}. In addition, a signal appeared at 1658 cm^{-1} when the intermolecular interaction occurred between the OH and C═O groups of PVP. Furthermore, Fig. 6(d) indicates that the fraction of hydrogen-bonded signals from the poly(S–*alt*–*p*HPMI)/PVP binary blends ($k = 1$; $q = 45$) was also higher than that from the poly(S–*alt*–DMHPMI)/PVP binary blends; this trend was similar to that in the PS–*alt*–PHPMIs/P4VP binary blends, but the fractions were both higher than those for the P4VP blends. The difference between the positive or negative deviation was that the intermolecular interactions in the PS–*alt*–PHPMIs/PVP binary blends were stronger than those in the PS–*alt*–PHPMIs/P4VP binary blends. Finally, we would expect the values of K_B for HPMI derivatives to be between 1200 and 6000 for the negative and positive values of q for the P4VP and PVP blends, respectively.

4. Conclusion

We have synthesized the monomer DMHPMI in three steps and then used it to form alternating poly(S–*alt*–DMHPMI) copolymers through free radical copolymerization with styrene. We used FTIR and NMR spectroscopy and MALDI-TOF mass spectrometry to confirm the chemical structure of the copolymer. A single value of T_g appeared for each PS–*alt*–PHPMI/P4VP blend composition, as measured using DSC, revealing full miscibility in the amorphous phase. A negative deviation from the linear rule appeared for the PS–*alt*–PHPMI/P4VP blends, due to weak acidity of both HPMI units, with the intermolecular interactions of poly(S–*alt*–DMHPMI) being weaker relatively to those in the other copolymer because of steric effects. FTIR spectral analyses of the ratio of hydrogen-bonded OH groups and pyridyl units reached the same conclusion. We also found a slightly positive deviation from the linear rule for the poly(S–*alt*–DMHPMI)/PVP blends, where the intermolecular interactions were also weaker than those in the poly(S–*alt*–*p*HPMI)/PVP blends, as would be expected because the values of K_B of the DMHPMI and *p*HPMI unit were between 1200 and 6000.

CRediT authorship contribution statement

Wei-Ting Du: Conceptualization, Data curation, Writing – original draft. **Tzu-Ling Ma:** Formal analysis, Data curation, Writing – original draft. **Shiao-Wei Kuo:** Funding acquisition, Project administration, Supervision, Writing.

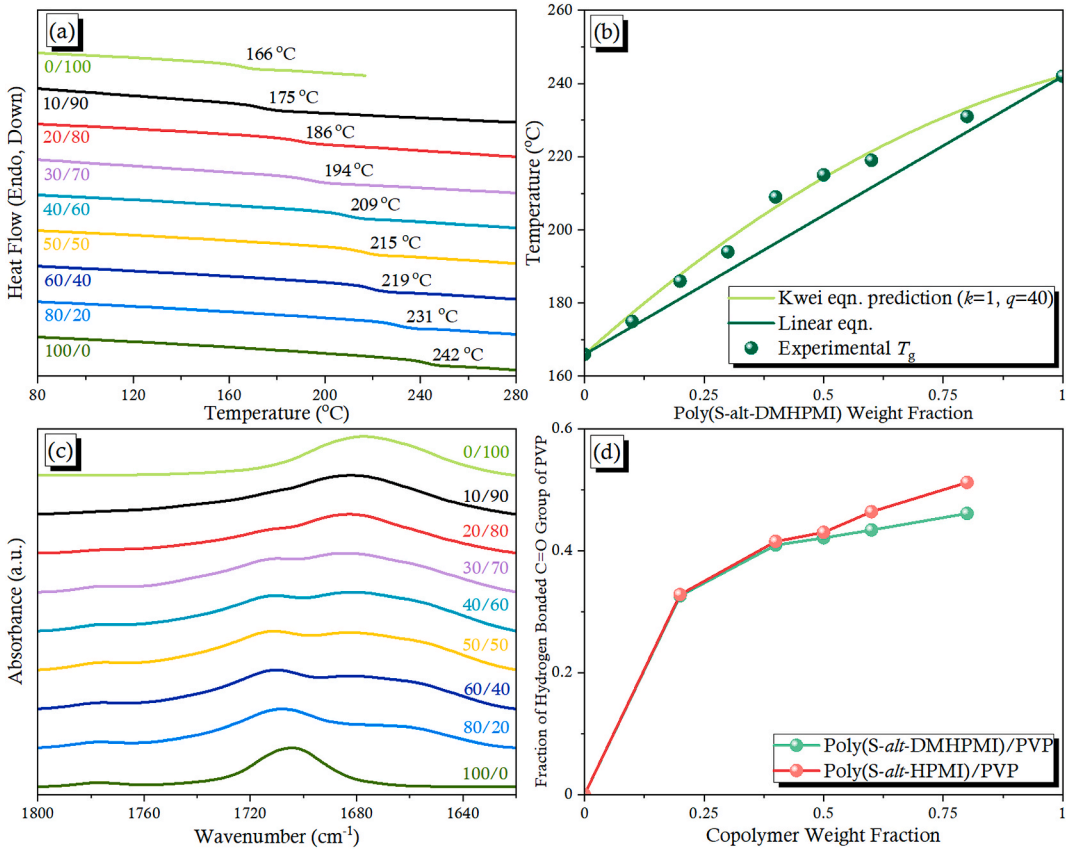

Fig. 6. (a) DSC thermal analyses of poly(S–*alt*–DMHPMI)/PVP binary blends of various weight ratios. (b) Corresponding values of T_g predicted by the linear rule and the Kwei equation for the poly(S–*alt*–DMHPMI)/PVP binary blends. (c) C═O group stretching region of the FTIR spectra of poly(S–*alt*–DMHPMI)/PVP binary blends, recorded at 25 °C after removing moisture. (d) Fraction of hydrogen-bonded C═O groups of PVP.

Declaration of competing interest

The authors declare that they have no known competing financial interests or personal relationships that could have appeared to influence the work reported in this paper.

Data availability

No data was used for the research described in the article.

Acknowledgments

This study was supported financially by the Ministry of Science and Technology, Taiwan, under contracts NSTC 110-2124-M-002-013 and 111-2223-E-110-004.

Appendix A. Supplementary data

Supplementary data to this article can be found online at https://doi.org/10.1016/j.polymer.2023.125694.

References

[1] S. Attar, B. Chen, G. Cicala, G. Catalanotti, T. Scalici, B.G. Falzon, On the mechanical properties of melt-blended nylon 6/ethylene-octene copolymer/graphene nanoplatelet nanocomposites, Polymer 243 (2022), 124619.
[2] M.J. Akanbi, S.N. Jayasinghe, A. Wojcik, Characterisation of electrospun PS/PU polymer blend fibre mat for oil sorption, Polymer 212 (2021), 123129.
[3] P. Parashar, K. Ramakrishna, A.T. Ramaprasad, A study on compatibility of polymer blends of polystyrene/poly(4-vinylpyridine), J. Appl. Polym. Sci. 120 (2011) 1729.
[4] S.W. Kuo, Hydrogen bonding mediated self-assembled structures from block copolymer mixtures to mesoporous materials, Polym. Int. 71 (2022) 393–410.
[5] T.C. Tseng, S.W. Kuo, Hydrogen-bonding strength influences hierarchical self-assembled structures in unusual miscible/immiscible diblock copolymer blends, Macromolecules 51 (2018) 6451.
[6] E.L. Lin, W.L. Hsu, Y.W. Chiang, Trapping structural coloration by a bioinspired gyroid microstructure in solid state, ACS Nano 12 (2018) 485–493.
[7] J.L. Swartz, B.R. Elling, I. Castano, M.P. Thompson, D.T. Sheppard, N. C. Gianneschi, W.R. Dichtel, Copolymers prepared by exchange reactions enhance the properties of miscible polymer blends, Macromolecules 55 (2022) 8548–8555.
[8] H.J. Kim, X. Peng, Y. Shin, M.A. Hillmyer, C.J. Ellison, Blend miscibility of poly (ethylene terephthalate) and aromatic polyesters from salicylic acid, J. Phys. Chem. B 125 (2021) 450–460.
[9] A.P.A. Carvalho, A.S. Sirqueira, Effect of compatibilization in situ on PA/SEBS blends, Polímeros 26 (2016) 123–128.
[10] S.W. Kuo, F.C. Chang, Miscibility and hydrogen bonding in blends of poly (vinylphenol-co-methyl methacrylate) with poly (ethylene oxide), Macromolecules 34 (2001) 4089–4097.
[11] P.J. Flory, Thermodynamics of heterogeneous polymers and their solutions, J. Chem. Phys. 12 (1944) 425.
[12] P.J. Flory, Statistical mechanics of linear association equilibria, J. Chem. Phys. 14 (1946) 49.
[13] G.C. Pimentel, A.L. McClellan, The Hydrogen Bond, WH Freeman, 1960.
[14] S.J. Grabowski, Hydrogen bonding strength—measures based on geometric and topological parameters, J. Phys. Org. Chem. 17 (2004) 18–31.
[15] S.W. Kuo, Hydrogen Bonding in Polymeric Materials, John Wiley & Sons, 2018.
[16] S. Zhang, P.C. Painter, J. Runt, Dynamics of polymer blends with intermolecular hydrogen bonding: broad-band dielectric study of blends of poly(4-vinyl phenol) with poly(vinyl acetate) and EVA70, Macromolecules 35 (2002) 8478–8487.
[17] J.J. Sotele, V. Soldi, A.T.N. Pires, Characterization and morphology of Novolak or poly(vinyl phenol)/poly(ethylene oxide) blends, Polymer 38 (1997) 1179–1185.
[18] P. Gestoso, J. Brisson, Investigation of the effect of chain rigidity on orientation of polymer blends: the case of poly(vinyl phenol)/poly(ethylene terephthalate) blends, Polymer 44 (2003) 7765–7776.
[19] J. Dai, S.H. Goh, S.Y. Lee, K.S. Siow, Complexation between poly(hydroxyether of bisphenol-A) and three tertiary amide polymers, Polymer 37 (1996) 3259–3264.
[20] S.W. Kuo, C.L. Lin, F.C. Chang, The study of hydrogen bonding and miscibility in poly(vinylpyridines) with phenolic resin, Polymer 43 (2002) 3943–3949.
[21] J. Hong, S.H. Goh, S.Y. Lee, K.S. Siow, Miscibility of poly(pvinylphenol) with poly (dialkyl itaconate)s and poly(methoxycarbonylmethyl methacrylate), Polymer 36 (1995) 143–147.
[22] M.M. Coleman, G.J. Pehlert, P.C. Painter, Functional group accessibility in hydrogen bonded polymer blends, Macromolecules 29 (1996) 6820–6831.
[23] S.W. Kuo, C.H. Wu, F.C. Chang, Thermal properties, interactions, morphologies, and conductivity behavior in blends of poly(vinylpyridine)s and zinc perchlorate, Macromolecules 37 (2004) 192–200.
[24] M.W. Huang, S.W. Kuo, H.D. Wu, F.C. Chang, S.Y. Fang, Miscibility and hydrogen bonding in blends of poly (vinyl acetate) with phenolic resin, Polymer 43 (2002) 2479–2487.
[25] W.T. Du, E.A. Orabi, M.G. Mohamed, S.W. Kuo, Inter/intramolecular hydrogen bonding mediate miscible blend formation between near-perfect alternating Poly (styrene-*alt*-hydroxyphenylmaleimide) copolymers and Poly(vinyl pyrrolidone), Polymer 219 (2021), 123542.
[26] S.W. Kuo, F.C. Chang, Studies of miscibility behavior and hydrogen bonding in blends of poly(vinylphenol) and poly(vinylpyrrolidone), Macromolecules 34 (2001) 5224–5228.
[27] Y.R. Jheng, M.G. Mohamed, S.W. Kuo, Supramolecular interactions induce unexpectedly strong emissions from triphenylamine-functionalized polytyrosine blended with poly(4-vinylpyridine), Polymers 9 (2017) 503.
[28] L.C. Cesteros, E. Meaurio, I. Katime, Miscibility and specific interactions in blends of poly(hydroxy methacrylates) with poly(vinylpyridines), Macromolecules 26 (1993) 2323–2330.
[29] A. Prinos, A. Dompros, C. Panayiotou, Thermoanalytical and spectroscopic study of poly (vinyl pyrrolidone)/poly (styrene-co-vinyl phenol) blends, Polymer 39 (1998) 3011–3016.
[30] C.W. Chiou, Y.C. Lin, L. Wang, C. Hirano, Y. Suzuki, T. Hayakawa, S.W. Kuo, Strong screening effect of polyhedral oligomeric silsesquioxanes (POSS) nanoparticles on hydrogen bonded polymer blends, Polymers 6 (2014) 926–948.
[31] M.P. Uliana, B.M. Servilha, O. Alexopoulos, K.T. de Oliveira, C.F. Tormena, M.A. B. Ferreira, T.J. Brocksom, The Diels–Alder reactions of para-benzoquinone nitrogen-derivatives: an experimental and theoretical study, Tetrahedron 70 (2014) 6963–6973.
[32] M. Arivazhagan, J.S. kumar, Molecular structure, vibrational spectral assignments, HOMO–LUMO, MESP, Mulliken analysis and thermodynamic properties of 2,6-xylenol and 2,5-dimethyl cyclohexanol based on DFT calculation, Spectrochim. Acta Mol. Biomol. Spectrosc. 137 (2015) 490–502.
[33] W.T. Du, S.W. Kuo, Varying the sequence distribution and hydrogen bonding strength provides highly Heat-Resistant PMMA copolymers, Eur. Polym. J. 170 (2022), 111165.
[34] M.G. Mohamed, K.C. Hsu, J.L. Hong, S.W. Kuo, Unexpected fluorescence from maleimide-containing polyhedral oligomeric silsesquioxanes: nanoparticle and sequence distribution analyses of polystyrene-based alternating copolymer, Polym. Chem. 7 (2016) 135–145.
[35] L.R. Hutchings, P.P. Brooks, D. Parker, J.A. Mosely, S. Sevinc, Monomer sequence control via living anionic copolymerization: synthesis of alternating, statistical, and telechelic copolymers and sequence analysis by MALDI ToF mass spectrometry, Macromolecules 48 (2015) 610–628.
[36] X. Xia, T. Gao, F. Li, R. Suzuki, T. Isono, T. Satoh, Multidimensional control of repeating unit/sequence/topology for one-step synthesis of block polymers from monomer mixtures, J. Am. Chem. Soc. 144 (2022) 17905–17915.
[37] L. Ulmer, J. Mattay, H.G. Torres-Garcia, H. Luftmann, Letter: the use of 2-[(2e)-3-(4-tert-butylphenyl)-2-methylprop-2-Enylidene]Malononitrile as a matrix for matrix-assisted laser desorption/ionization mass spectrometry, Eur. J. Mass Spectrom. 6 (2000) 49–52.
[38] M.M. Coleman, P.C. Painter, Hydrogen bonded polymer blends, Prog. Polym. Sci. 20 (1995) 1–59.
[39] S.W. Kuo, F.C. Chang, Effects of copolymer composition and free volume change on the miscibility of poly(styrene-co-vinylphenol) with poly(ε-caprolactone), Macromolecules 34 (2001) 7737–7743.
[40] J.J. Benvenuta-Tapia, E. Vivaldo-Lima, T. Tenorio-Lopez, M. Vargas-Hernandez, H. Vazquez-Torres, Kinetic analysis of the RAFT copolymerization of styrene and maleic anhydride by differential scanning calorimetry, Thermochim. Acta 667 (2018) 93–101.
[41] T. Kwei, The effect of hydrogen bonding on the glass transition temperatures of polymer mixtures, J. Polym. Sci. Polym. Lett. Ed. 22 (1984) 307–313.
[42] S.W. Kuo, P.H. Tung, F.C. Chang, Syntheses and the study of strongly hydrogen-bonded poly(vinylphenol-b-vinylpyridine) diblock copolymer through anionic polymerization, Macromolecules 39 (2006), 9388–9939.
[43] O. Urakawa, A. Yasue, Glass transition behaviors of poly (vinyl pyridine)/poly (vinyl phenol) revisited, Polymers 11 (2019) 1153.
[44] C.C. Huang, M.X. Du, B.Q. Zhang, C.Y. Liu, Glass transition temperatures of copolymers: molecular origins of deviation from the linear relation, Macromolecules 55 (2022) 3189–3200.
[45] W.T. Du, Y.L. Kuan, S.W. Kuo, Intra- and intermolecular hydrogen bonding in miscible blends of CO_2/epoxy cyclohexene copolymer with poly(vinyl phenol), Int. J. Mol. Sci. 23 (2022) 7018.
[46] S.W. Kuo, C.F. Huang, F.C. Chang, Study of hydrogen-bonding strength in poly (ε-caprolactone) blends by DSC and FTIR, J. Polym. Sci. Polym. Phys. Ed 39 (2001) 1348–1359.
[47] J. Wang, M.K. Cheung, Y. Mi, Miscibility in blends of poly (4-vinylpyridine)/poly (4-vinylphenol) as studied by 13C solid–state NMR, Polymer 42 (2001) 3087–3093.
[48] I. Noda, Y. Ozaki, Two-Dimensional Correlation Spectroscopy, John Wiley & Sons, Hoboken, NJ, USA, 2004.